Role of Co clusters in wurtzite Co:ZnO dilute magnetic semiconductor thin films

ARTICLE *in* JOURNAL OF APPLIED PHYSICS · MARCH 2009

Impact Factor: 2.18 · DOI: 10.1063/1.3074297 · Source: IEEE Xplore

9 AUTHORS, INCLUDING:

Zhiyun Pan
University of Science and Technology of China
78 PUBLICATIONS **701** CITATIONS
SEE PROFILE

Cong Mai
North Carolina State University
8 PUBLICATIONS **126** CITATIONS
SEE PROFILE

Zhihu Sun
University of Science and Technology of China
117 PUBLICATIONS **1,446** CITATIONS
SEE PROFILE

Yong Jiang
Southern Medical University
144 PUBLICATIONS **1,143** CITATIONS
SEE PROFILE

Role of Co clusters in wurtzite Co:ZnO dilute magnetic semiconductor thin films

He Wei, Tao Yao, Zhiyun Pan, Cong Mai, Zhihu Sun, Ziyu Wu,[a] Fengchun Hu, Yong Jiang, and Wensheng Yan

National Synchrotron Radiation Laboratory, University of Science and Technology of China, Hefei 230029, People's Republic of China

(Received 10 November 2008; accepted 16 December 2008; published online 17 February 2009)

The magnetic nature of $Zn_{1-x}Co_xO$ dilute magnetic semiconductor (DMS) thin films grown by pulsed laser deposition is investigated by x-ray absorption fine structure spectroscopy and x-ray diffraction. We show that a single phase of the substitutional Co atoms occupied Zn sites in the ZnO matrix exists in the $Zn_{0.98}Co_{0.02}O$ DMS thin film while a secondary phase of the Co clusters is formed in $Zn_{0.95}Co_{0.05}O$ and $Zn_{0.90}Co_{0.10}O$ thin films. Despite the formation of Co clusters, the average magnetic moment M_S per Co atom is sharply decreased with increasing Co concentration, which suggests that the small Co clusters are superparamagnetic. For the $Zn_{0.98}Co_{0.02}O$ DMS thin film, the local structural distortion around the substitutional Co atoms is interpreted as the origin of intrinsic weak room-temperature ferromagnetism. © *2009 American Institute of Physics*.
[DOI: 10.1063/1.3074297]

I. INTRODUCTION

Dilute magnetic semiconductors (DMSs) attracted much scientific attention due to their potential applications in spin-based electronic technologies.[1,2] Particularly, transition metal-doped ZnO DMSs with a predicted high Curie temperature (T_C) attract increasing interest.[3,4] A number of studies reported room-temperature (RT) ferromagnetism behavior in Co-doped ZnO DMSs by employing different fabrication techniques including molecular-beam epitaxy,[5] pulsed laser deposition (PLD),[4] magnetron sputtering,[6] sol-gel preparation,[7] etc. Up to date, the origin of ferromagnetic behaviors, particularly a possibility arising from either the intrinsic phenomenon[3,4] or the second phase such as Co clusters[7,8] in Co doped ZnO, remains controversial in literatures.

To interpret the origin of the magnetic properties of DMSs, various magnetic interaction mechanisms have been proposed, including RKKY, direct superexchange, indirect superexchange, and double exchange mechanism.[9] Furthermore, numerous experiment results attributed the observed ferromagnetism to oxygen vacancies or cobalt clusters in insulated oxide-based DMSs.[4–8] Recently, it has been reported that the homogeneous DMSs with a low structural disorder inside the oxide matrix should exhibit a weak ferromagnetism.[10] The degree of structural disorder, both locally around the dopant and throughout the entire semiconductor, can have a profound effect on magnetic properties.[11,12] In general, the investigations on the structures of DMSs indicate that Co ions totally dissolved in the ZnO wurtzite lattice when Co doping concentration is low to about 5%.[13] For a high doping concentration larger than 10%, not all Co ions replace Zn sites and a part of them is separated to form a precipitate.[7] Thus, in order to clarify the origin of ferromagnetism, it is essential to determine the real structure around the Co ions in Co-doped ZnO DMSs. However, conventional x-ray diffraction (XRD) and transmission electron microscopy (TEM) techniques have difficulty in detecting the small amount of precipitates, such as Co compounds or Co metal in Co-doped ZnO DMSs.[14] Fortunately, x-ray absorption fine structure (XAFS) technique, with its sensitivity to the low concentration and local structure, has been successfully used to identify Co-metal clusters,[7] Co_3O_4 precipitates,[15] and the substitutional Co atoms in Zn sites.[16]

In this work, XAFS and XRD were combined to investigate the atomic structure in $Zn_{1-x}Co_xO$ thin films with RT ferromagnetism. We aim to determine the dependence of magnetism feature on the local structure around the Co atoms and the formation of the secondary phase. The results show that in $Zn_{0.98}Co_{0.02}O$ thin film all of the Co atoms substitute Zn atoms in the wurtzite structure of ZnO, while a small proportion of Co atoms is precipitated to form metallic clusters in $Zn_{0.95}Co_{0.05}O$ and $Zn_{0.90}Co_{0.10}O$ thin films. The magnetic behavior suggests that the RT ferromagnetism is really induced by the local structural distortion and the smaller Co clusters show a superparamagnetic property in the $Zn_{1-x}Co_xO$ thin films.

II. EXPERIMENTAL DETAILS

The $Zn_{1-x}Co_xO$ thin films with a thickness of about 100 nm were grown on Si (100) substrates by the PLD method. Targets were prepared by standard ceramic procedures from ZnO and CoO powders of 4*N* purity with stoichiometric amounts $x=0.02$, 0.05, 0.10. A KrF excimer laser (LAMBDA PHYSIK LPX 200) with a wavelength of 248 nm was used for the deposition. The repetition rate is 5 Hz and the laser energy density is 150 mJ/pulse. The deposition chamber was evacuated to a base pressure lower than 1×10^{-4} Pa and the $Zn_{1-x}Co_xO$ thin films were deposited at the substrate temperature of 923 K.

[a]Authors to whom correspondence should be addressed. Electronic address: wuzy@ustc.edu.cn.

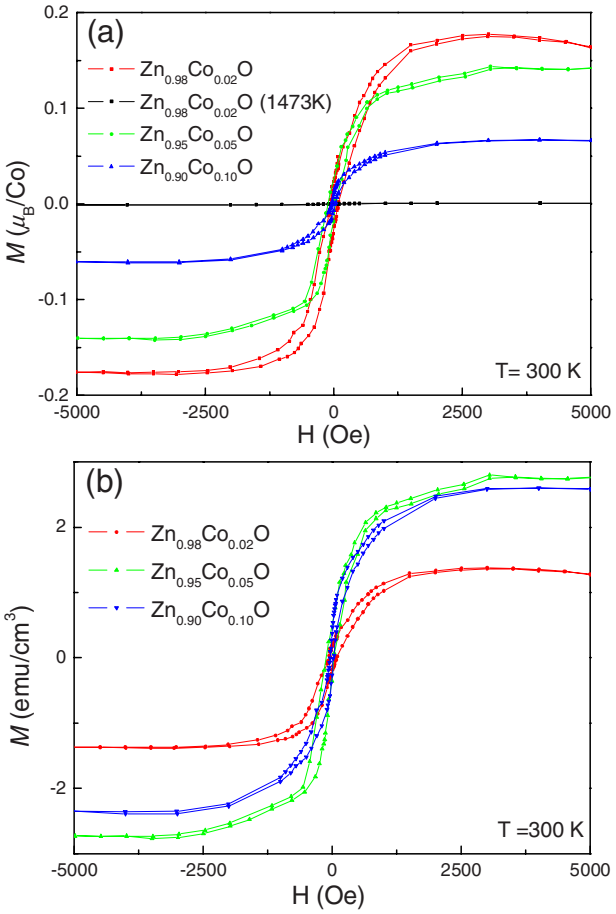

FIG. 1. (Color online) The RT *M-H* curves for the $Zn_{1-x}Co_xO$ (x=0.02, 0.05, and 0.10) thin films, the $Zn_{0.98}Co_{0.02}O$ (1473 K) powder as reference. (a) The average magnetic moment (μ_B) per Co atom (μ_B/Co). (b) emu per cubic centimeter (emu/cm^3).

The sample quality of the $Zn_{1-x}Co_xO$ thin films was studied by XRD (θ-2θ scans) using an x-ray diffractometer with Cu $K\alpha$ radiation. A superconducting quantum interference device was used to measure the magnetic property. The magnetic field ranging from −5000 to 5000 Oe was applied parallel to the surface of the thin films. The Co *K*-edge XAFS spectra of the $Zn_{1-x}Co_xO$ thin films were measured at the U7C beamline of the National Synchrotron Radiation Facility (NSRL), China and the BL-13B1 beamline of Photon Factory (PF) of the High Energy Accelerator Research Organization, Japan. The electron-beam energy of NSRL was 0.8 GeV and the maximum stored current was about 250 mA. The electron-beam energy of PF was 2.5 GeV and the maximum stored current was about 450 mA. The Si (111) plane double-crystal monochromator and high purity 7-element and 100-element Ge array detectors were used.[17] The energy resolution was better than 2 eV at 9 keV, calibrated from the near-edge features of copper metal at the Fermi energy E_f (8.9803 keV). XAFS data were analyzed by USTCXAFS3.0 software packages compiled by Zhong and Wei[18] according to standard procedures.

III. RESULTS

Figure 1 demonstrates the RT *M-H* curves for the $Zn_{1-x}Co_xO$ thin films and the $Zn_{0.98}Co_{0.02}O$ (annealed at 1473 K in air) powder as reference, where the average magnetic moment (μ_B) per Co atom [Fig. 1(a)] and emu per cubic centimeter [Fig. 1(b)] are displayed, respectively. The well-defined hysteresis loop can be clearly observed for all doped thin films except the paramagnetic property for the $Zn_{0.98}Co_{0.02}O$ (1473 K) powder, indicating the RT ferromagnetism behavior for the PLD-grown thin films. The saturation magnetic moment (M_S) decreases from 0.18 to 0.13 and 0.05 μ_B/Co with increasing Co concentration from 0.02 to 0.05 and 0.10. However, the curves of M (emu/cm^3)-H show an obvious reverse trend. The M_S is almost 2.6 emu/cm^3 for $Zn_{0.90}Co_{0.10}O$ and $Zn_{0.95}Co_{0.05}O$ thin films, and this is much larger than that (1.2 emu/cm^3) of the $Zn_{0.98}Co_{0.02}O$ thin film. The underlying magnetic mechanism will be discussed later.

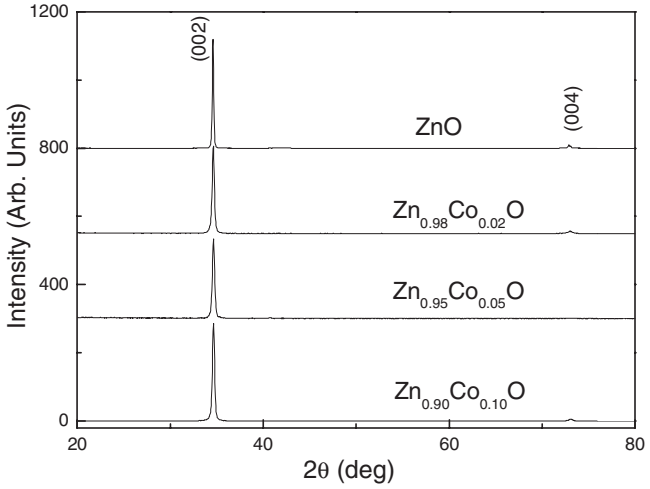

FIG. 2. The XRD patterns of $Zn_{1-x}Co_xO$ thin films and the reference ZnO thin film.

The XRD patterns of $Zn_{1-x}Co_xO$ thin films and the reference ZnO thin film are shown in Fig. 2. Only two peaks located at 34.6° and 72.9° are the characteristic of the hexagonal wurtzite ZnO ([002] and [004] crystalline faces). No extra diffraction peaks from any Co-related secondary phases or impurities can be detected in the XRD patterns. This indicates that these $Zn_{1-x}Co_xO$ thin films show a good crystallinity with a wurtzite structure and a *c*-axis preferred orientation.[19] However, since the XRD method is not sensitive enough to detect nanoscale precipitates, further characterization is necessary to obtain the detailed structure information.

Figures 3(a) and 3(b) display the Co *K*-edge extended XAFS (EXAFS) oscillation functions $k^3\chi(k)$ and their Fourier transforms (FTs) for $Zn_{1-x}Co_xO$ thin films. As references, the Co *K*-edge functions of $Zn_{0.98}Co_{0.02}O$ (1473 K) powder, Co foil, CoO, Co_3O_4, and Zn *K*-edge result of ZnO are also plotted. One can see that the existence of the CoO and Co_3O_4 can be safely excluded, since their $k^3\chi(k)$ and FT features are significantly different from those of $Zn_{1-x}Co_xO$ thin films and $Zn_{0.98}Co_{0.02}O$ powder. Figure 3(a) manifests that the oscillation shapes of the $Zn_{0.98}Co_{0.02}O$ thin film and powder are quite similar to that of ZnO. With increasing Co content, the oscillations of $Zn_{1-x}Co_xO$ (x=0.05 and 0.10) thin films show evident change in the regions of 5–7 and

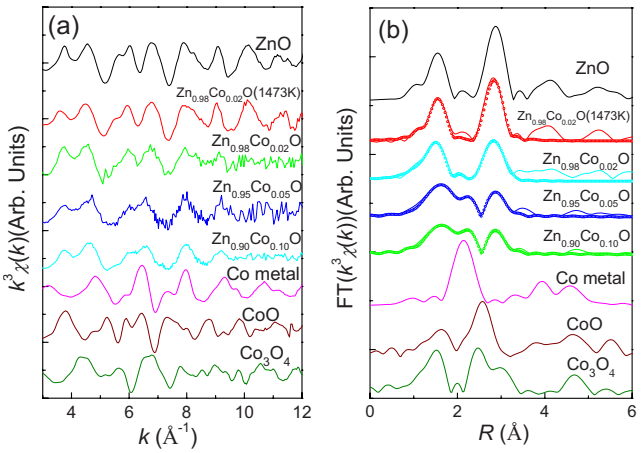

FIG. 3. (Color online) (a) The Co *K*-edge EXAFS oscillation functions $k^3\chi(k)$ for the $Zn_{1-x}Co_xO$ thin films, the $Zn_{0.98}Co_{0.02}O$ (1473 K) powder, Co foil, CoO and Co_3O_4 powders, as well as the Zn *K*-edge function for ZnO thin film. (b) Their FTs spectra. The empty circles show the fitting results.

10–12 $Å^{-1}$, implying a different local environment surrounds Co atoms. In addition, the FT of $Zn_{0.98}Co_{0.02}O$ thin film and powder shown in Fig. 3(b) are close to that of pure ZnO, presenting two strong peaks at around 1.6 and 2.8 Å. This reveals that all the Co ions occupy the Zn sites in the ZnO lattice both in the thin film and the powder at a low Co doping concentration. However, one can easily observe that the intensities of the first nearest neighbor Co–O pair and the second nearest neighbor Co–Zn pair for the $Zn_{0.98}Co_{0.02}O$ thin film are much lower than those of the ZnO. This implies that the disorder degree around the Co atoms is large in the $Zn_{0.98}Co_{0.02}O$ thin film. At the Co doping concentration x of 0.05, the corresponding Co–O and Co–Zn peaks remain in existence, but the first peak is obviously broadened and a new small peak as the characteristic peak of metallic Co appears at 2.15 Å. Increasing x to 0.10, the intensity of the peak increases strongly. It is clear that, at Co concentration $x \geq 0.05$, not all the Co ions are incorporated into the lattice of wurtzite ZnO, and part of them is separated to form the Co clusters. Therefore, we can conclude that in $Zn_{0.95}Co_{0.05}O$ and $Zn_{0.90}Co_{0.10}O$ thin films, most of Co atoms substitute the Zn sites while a part of Co atoms forms the precipitate of Co clusters. Similar result has been found in $Zn_{1-x}Co_xO$ thin films prepared by the sol-gel method.[7] The ratio of Co atoms in the substitutional site to those in the Co clusters could be further obtained from EXAFS fitting results.

In order to obtain quantitative structural information, we fitted the main peaks including the Co–O and Co–Co pairs. Since the Co atoms in the $Zn_{0.98}Co_{0.02}O$ thin film only occupy Zn sites, the coordination number of the Co–O pair is close to four. To simplify our model, in $Zn_{0.95}Co_{0.05}O$ and $Zn_{0.90}Co_{0.10}O$ thin films, the coordination numbers of Co–O and Co–Co pairs were set as $4(1-p)$ and $12p$, respectively, $(0<p<1)$, where p is denoted as the percentage of Co clusters in $Zn_{1-x}Co_xO$ thin films. From the basic formula of EXAFS,[20] the best fitting structural parameters obtained for all the $Zn_{1-x}Co_xO$ thin films are summarized in Table I and the curve fitting results are shown as empty circles in Fig. 3.

IV. DISCUSSION

The EXAFS results have clearly shown that the Co atoms are homogeneously incorporated into the ZnO lattice and only a single phase appears in the $Zn_{0.98}Co_{0.02}O$ thin film with low Co doping concentration of 0.02, while a major proportion of substitutional Co atoms and small amount of cobalt clusters coexist in the $Zn_{0.95}Co_{0.05}O$ and $Zn_{0.90}Co_{0.10}O$ thin films with a high doping concentration. From the EXAFS results listed in Table I, we obtained that about 25% and 40% Co dopants form Co clusters in $Zn_{0.95}Co_{0.05}O$ and $Zn_{0.90}Co_{0.10}O$ thin films, respectively. Therefore, the distribution of Co atoms and the ratio of various Co phases in the $Zn_{1-x}Co_xO$ thin films grown by the PLD method at 923 K, strongly depend on the concentration of the Co dopant. For the $Zn_{0.95}Co_{0.05}O$ and $Zn_{0.90}Co_{0.10}O$ thin films, the concentrations of Co atoms in the substitutional site are 0.037 and 0.060, respectively, indicating that, in the $Zn_{1-x}Co_xO$ thin films, the solubility of Co atoms in ZnO is largely affected by the total Co doping concentration.

For the $Zn_{0.98}Co_{0.02}O$ thin film grown by PLD, the bond length R_{Co-O} and Debye–Waller factor σ^2_{Co-O} in the first nearest neighbor around the Co atoms are 1.99 Å and 4.1×10^{-3} $Å^2$, respectively. The results show that the local structure of Co atoms in the ZnO lattice is expanded and distorted, compared to that in the pure ZnO (the $R_{Zn-O}=1.97$ Å, $\sigma^2_{Zn-O}=1.8\times10^{-3}$ $Å^2$) and that in the $Zn_{0.98}Co_{0.02}O$ powder annealed at 1473 K ($R_{Zn-O}=1.98$ Å, $\sigma^2_{Zn-O}=2.2\times10^{-3}$ $Å^2$). The phenomena of local expansion and distortion in the first Co–O shell has also been reported for the $Zn_{1-x}Co_xO$ thin films grown by PLD method at 673 K with much higher Co doping concentration of 26%,[16] where the R_{Co-O} and σ^2_{Co-O} are 1.98 Å and 4.0×10^{-3} $Å^2$, respectively. In the previous investigation, we obtained that the

TABLE I. Structure parameters around Co atoms in $Zn_{1-x}Co_xO$ thin films.

Sample	Coordination	p [a]	Coordination numbers (N)	R_{eff} (Å)	R (Å)	σ^2 ($Å^2$)
ZnO	Zn–O	···	4	1.97	1.97±0.02	0.0018±0.0008
Co	Co–Co	···	12	2.50	2.50±0.03	0.0061±0.0015
$Zn_{0.98}Co_{0.02}O$	Co–O	···	~4		1.99±0.01	0.0041±0.0007
$Zn_{0.95}Co_{0.05}O$	Co–O	···	~4		1.99±0.02	0.0038±0.0010
	Co–Co	25%	~12		2.51±0.01	0.0073±0.0018
$Zn_{0.90}Co_{0.10}O$	Co–O	···	~4		1.99±0.01	0.0040±0.0011
	Co–Co	40%	~12		2.52±0.01	0.0075±0.0017

[a] p is the percentage of Co cluster in $Zn_{1-x}Co_xO$ thin films.

R_{Co-O} and σ^2_{Co-O} are 1.99 and 2.1×10^{-3} Å^2 for $Zn_{0.98}Co_{0.02}O$ nanocomposites prepared by the sol-gel method.[15] It implies that the fabrication by PLD at the growth temperature of 923 K favors to grow a $Zn_{0.98}Co_{0.02}O$ thin film with a large disorder in the local structure around Co atoms. Hence, we consider that the local distortion around Co atoms is mainly determined by the preparation methods and growth conditions.

From the magnetic properties shown in Fig. 1, all the thin films show a weak RT ferromagnetism with a magnetic moment between 0.18 and 0.05 μ_B/Co. The value of their M_S is similar to those reported in the previous literatures.[3,7] Interestingly, we can find the noncorrelation between the Co ion concentrations and the saturation magnetizations M_S for the $Zn_{1-x}Co_xO$ thin films. The M_S of saturation magnetic moment per Co atom decreases to about 72% and 28% of that in $Zn_{0.98}Co_{0.02}O$ for the Co doping concentration of 5% and 10%, respectively. A similar result for the $Zn_{1-x}Co_xO$ thin films has been found by Venkatasan *et al.*,[21] who consider that the decrease in M_S is due to the increase in the antiferromagnetic coupling of Co ion pairs and groups with the Co concentration. Our recent XAFS results further confirmed that the substitutional Co ions in ZnO tend to gather together.[22] It strongly suggests that the magnetic properties for the $Zn_{1-x}Co_xO$ thin films cannot be simply rationalized in terms of the random distribution of Co^{2+} spin moment at Zn sites. For the $Zn_{0.95}Co_{0.05}O$ and $Zn_{0.90}Co_{0.10}O$ thin films, the proportion of Co clusters is 25% and 40%, and the concentration of the substitutional Co atoms is 0.037 and 0.060, respectively. Indirect superexchange interaction of Co^{2+} between large distance is expected to lead to ferromagnetism, whereas the short-range superexchange interaction of Co ion pairs or groups is predominantly antiferromagnetically coupled.[1,4] Therefore, the average magnetic moment M_S per substitutional Co atom is decreased by the antiferromagnetic coupling of Co ion pairs and groups in the $Zn_{1-x}Co_xO$ thin films with high doping concentration x. Besides, the formation of Co clusters has been observed in $Zn_{0.95}Co_{0.05}O$ and $Zn_{0.90}Co_{0.10}O$ thin films. To understand the ferromagnetic nature of these DMSs, we should consider the ferromagnetic contributions from the substitutional Co atoms and the Co clusters for the $Zn_{1-x}Co_xO$ thin films in detail.

The Co clusters with the size of about 10 nm, observed by means of high-resolution TEM (HRTEM), have been regarded as the origin of the ferromagnetism for the Co-doped ZnO (Ref. 7) and TiO_2 thin films.[23] The magnetization measurements demonstrate the M_S 1.7 μ_B per Co atom for Co cluster.[23] Liu *et al.*[24] found the formation of the 4.5 nm Co nanodots embedded inside ZnO from their HRTEM images and reported that the value of M_S is 1.1 μ_B/Co. Similarly, Norton *et al.*[25] showed that the diffraction peaks corresponding to Co nanocrystals with the size of 3.5 nm appear in the XRD pattern of Co-doped ZnO thin films, however, the Co nanocrystals in Co-implanted ZnO single crystals demonstrate a superparamagnetic property at 300 K. The theoretical studies by Vargas *et al.*[26] indicated that small Co clusters may have no ferromagnetism at RT due to a pronounced temperature dependence on magnetization. The magnetism of small Co cluster is largely influenced by the size and temperature, namely, the saturation magnetization will be decreased remarkably with the reduced size and the increased temperature. These results suggest that the large Co clusters lead to the ferromagnetism but the small ones are superparamagnetic and exhibit no hysteresis curve at RT.

Since no peaks of Co nanocrystals can be detected by XRD as shown in Fig. 2, the grain sizes of Co clusters existing in the $Zn_{0.95}Co_{0.05}O$ and $Zn_{0.90}Co_{0.10}O$ thin films confirmed by XAFS should be very small, much below 3.5 nm.[25,27] Based on the above discussions, it is easy to conclude that the small Co clusters in the PLD-grown $Zn_{0.95}Co_{0.05}O$ and $Zn_{0.90}Co_{0.10}O$ thin films are superparamagnetic. Comparing with previous reported results,[23–25] the M_S of such a small Co cluster will be decreased by about several times at RT and approximates 0.1 μ_B/Co, which is much lower than that of the $Zn_{0.98}Co_{0.02}O$ thin film (0.18 μ_B/Co). Thus, we consider that two reasons, superparamagnetic Co clusters and the antiferromagnetic coupling of Co ion pairs, result in the decrease in the average magnetic moment per Co atom in the $Zn_{0.95}Co_{0.05}O$ and $Zn_{0.90}Co_{0.10}O$ thin films, compared to the M_S per Co atom in the $Zn_{0.98}Co_{0.02}O$ thin film. It is also reasonable that, for the $Zn_{0.95}Co_{0.05}O$ and $Zn_{0.90}Co_{0.10}O$ thin films, their M_S (emu/cm^3) is larger than that of $Zn_{0.98}Co_{0.02}O$ films [Fig. 1(b)] due to the increase in effective Co^{2+} concentration in these two samples.

As discussed above, the Co clusters with a smaller size in the $Zn_{0.95}Co_{0.05}O$ and $Zn_{0.90}Co_{0.10}O$ thin films are superparamagnetic, thus it cannot be used to explain the observed RT ferromagnetism origin of $Zn_{1-x}Co_xO$ DMS. Furthermore, XAFS and XRD results indicated that the $Zn_{0.98}Co_{0.02}O$ thin film is a single phase and Co ions are completely incorporated into the ZnO matrix. Therefore, we consider that the weak RT ferromagnetism (0.18 μ_B/Co) in $Zn_{0.98}Co_{0.02}O$ thin film is intrinsic and is related to the substitutional Co atoms at the Zn sites of ZnO lattice. In fact, there are currently two viewpoints in interpreting ferromagnetic mechanism of the substitutional Co atoms in the $Zn_{1-x}Co_xO$ thin films. One is the local lattice distortion around the Co atoms and the other is the formation of bound magnetic polarons by oxygen vacancies.[1,4]

Recently, a number of studies have shown the intrinsically paramagnetic properties for the $Zn_{1-x}Co_xO$ DMSs with a perfect structure.[28,29] Yin *et al.*[28] have shown that the bulk polycrystalline $Zn_{0.90}Co_{0.10}O$ DMS synthesized under high pressure (6 GPa) and high temperature (1273 K) is paramagnetic at RT. This is identical with our $Zn_{0.98}Co_{0.02}O$ (1473 K) powder, which presents a paramagnetism of 0.0008 μ_B per Co atom as shown Fig. 1. Also, Chambers and co-workers[29] have shown that, in their $Zn_{0.90}Co_{0.10}O$ thin film with high structural perfection, the magnetic behavior is purely paramagnetic at RT. Different from these reports, the local structure around Co atoms is largely distorted in our PLD-grown $Zn_{1-x}Co_xO$ thin films grown at 923 K. Hence, the observed RT ferromagnetism of $Zn_{0.98}Co_{0.02}O$ thin films as shown in Fig. 1 is likely correlated with this structural distortion.

Oxygen vacancies (O_V) have been considered to play an important role in the origin of RT ferromagnetism for oxide DMSs.[4,5] The x-ray absorption near edge structure (XANES) technique has been successfully used to identify the exis-

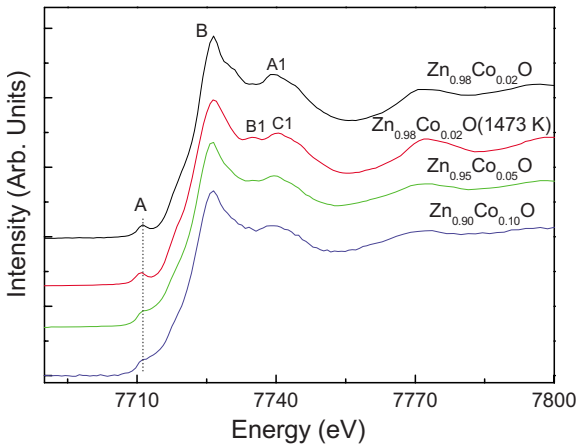

FIG. 4. (Color online) The Co *K*-edge XANES spectra of $Zn_{1-x}Co_xO$ thin films and the $Zn_{0.98}Co_{0.02}O$ (1473K) powder.

tence or absence of oxygen vacancy in Co-doped ZnO DMS.[15] The Co *K*-edge XANES spectra of $Zn_{1-x}Co_xO$ thin films and the $Zn_{0.98}Co_{0.02}O$ (1473 K) powder are shown in Fig. 4. Obviously, the intensity in the "valley" between the pre-edge $1s-3d$ feature (peak *A*) and the white line peak (peak *B*) for $Zn_{0.95}Co_{0.05}O$ and $Zn_{0.90}Co_{0.10}O$ thin films is significantly increased compared to that for the $Zn_{0.98}Co_{0.02}O$ thin film and the powder. This is due to the presence of numerous metallic Co in $Zn_{0.95}Co_{0.05}O$ and $Zn_{0.90}Co_{0.10}O$ thin films.[30] From Fig. 4, it can be clearly seen that the $Zn_{0.98}Co_{0.02}O$ (1473 K) powder presents the feature of two postedge double-peaks located at *B*1 (7735 eV) and *C*1 (7740 eV), indicating the absence of O_V. However, in the $Zn_{0.98}Co_{0.02}O$ thin film, only one peak *A*1 (7739 eV) exactly represents the XANES characteristic with O_V. This is a powerful witness to the existence of oxygen vacancies in our $Zn_{1-x}Co_xO$ thin films. Taking the above EXAFS results into account, the local structural disorder around Co in the $Zn_{1-x}Co_xO$ thin films can be interpreted from another aspect in terms of the formation of O_V. This magnetic explanation resembles the RT ferromagnetism in nanoparticles of nonmagnetic oxides such as HfO_2 and ZnO. For example, Potzger *et al.*[31] considered that the ferromagnetism in pure ZnO is due to the creation of defect (O_V) in the process of mechanical force. Therefore, the detailed analysis of magnetism and structure leads us to conclude that the oxygen vacancies induced by local lattice distortion is the origin of the RT ferromagnetism in the $Zn_{1-x}Co_xO$ DMS thin films grown by the PLD method.

V. CONCLUSION

The XAFS and XRD techniques have been used to investigate the structures of $Zn_{1-x}Co_xO$ ($x=0.02$, 0.05, and 0.10) thin films prepared by PLD. The EXAFS analysis of Co *K*-edge reveals that all of the Co ions are substantially incorporated into the lattice of ZnO for the $Zn_{0.98}Co_{0.02}O$ thin film as expected. However, a secondary phase of Co clusters is formed in the $Zn_{0.95}Co_{0.05}O$ and $Zn_{0.90}Co_{0.10}O$ thin films as seen from the Co *K*-edge EXAFS spectra, which is not detected by XRD. Magnetization measurement indicates that the RT ferromagnetism appears in all the thin films and the magnetic moment per Co atom is decreased with Co concentration. These lead us to conclude that the small Co clusters are superparamagnetic and decrease the average magnetic moment M_S per Co atom in the $Zn_{1-x}Co_xO$ DMS thin films for the dopant contents of 0.05 and 0.10. The local lattice distortion and oxygen vacancies around the Co atoms play a key role on the observed intrinsic RT ferromagnetism in the $Zn_{0.98}Co_{0.02}O$ DMS thin film.

ACKNOWLEDGMENTS

This work was supported by the National Natural Science Foundation of China (Grant Nos. 10605024, 10635060, 20621061, and 10725522). The authors would like to thank NSRL and KEK-PF for the synchrotron radiation beamtime.

[1]T. Dietl, H. Ohno, F. Matsukura, J. Cibert, and D. Ferrand, Science **287**, 1019 (2000).
[2]D. D. Awschalom and M. E. Flatte, Nat. Phys. **3**, 153 (2007).
[3]K. R. Kittilstved, D. A. Schwartz, A. C. Tuan, S. M. Heald, S. A. Chambers, and D. R. Gamelin, Phys. Rev. Lett. **97**, 037203 (2006).
[4]J. M. D. Coey, M. Venkatesan, and C. B. Fitzgerald, Nature Mater. **4**, 173 (2005).
[5]G. L. Liu, Q. Cao, J. X. Deng, P. F. Xing, Y. F. Tian, Y. X. Chen, S. S. Yan, and L. M. Mei, Appl. Phys. Lett. **90**, 052504 (2007).
[6]H. S. Hsu, J. C. A. Huanget, Y. H. Huang, Y. F. Liao, M. Z. Lin, C. H. Lee, J. F. Lee, S. F. Chen, L. Y. Lai, and C. P. Liu, Appl. Phys. Lett. **88**, 242507 (2006).
[7]J. H. Park, M. G. Kim, H. M. Jang, S. W. Ryu, and Y. M. Kim, Appl. Phys. Lett. **84**, 1338 (2004).
[8]J. H. Kim, H. Kim, D. Kim, Y. E. Ihm, and W. K. Choo, J. Appl. Phys. **92**, 6066 (2002).
[9]C. Liu, F. Yun, and H. Morkoc, J. Mater. Sci. **16**, 555 (2005).
[10]B. D. Yuhas, S. Fakra, M. A. Marcus, and P. D. Yang, Nano Lett. **7**, 905 (2007).
[11]B. Lee, X. Cartoixà, N. Trivedi, and R. M. Martin, Phys. Rev. B **76**, 155208 (2007).
[12]M. Berciu and R. N. Bhatt, Phys. Rev. Lett. **87**, 107203 (2001).
[13]K. Rode, R. Mattana, A. Anane, V. Cros, E. Jacquet, J.-P. Contour, F. Petroff, A. Fert, M. A. Arrio, P. Sainctavit, P. Bencok, F. Wilhelm, N. B. Brookes, and A. Rogalev, Appl. Phys. Lett. **92**, 012509 (2008).
[14]H.-J. Lee, Europhys. Lett. **72**, 76 (2005).
[15]T. F. Shi, S. Y. Zhu, Z. H. Sun, S. Q. Wei, and W. H. Liu, Appl. Phys. Lett. **90**, 102108 (2007).
[16]G. Martínez-Criadoa, A. Segura, J. A. Sans, A. Homs, J. P. Porres, and J. Susini, Appl. Phys. Lett. **89**, 061906 (2006).
[17]H. Oyanagi, C. Fonne, D. Gutknecht, P. Dressler, R. Henck, M. O. Lampert, S. Ogawa, K. Kasai, and S. B. Mohamed, Nucl. Instrum. Methods Phys. Res. A **513**, 340 (2003).
[18]W. J. Zhong and S. Q. Wei, J. Chin. Univ. Sci. Technol. **31**, 328 (2001).
[19]K. Shoji and Y. Uehara, Jpn. J. Appl. Phys., Part 1 **30**, 2315 (1991).
[20]Z. Y. Pan, Z. H. Sun, Z. Xie, J. H. Xu, I. Kojima, and S. Q. Wei, J. Phys. D **39**, 2796 (2006).
[21]M. Venkatesan, C. B. Fitzgerald, J. G. Lunney, and J. M. D. Coey, Phys. Rev. Lett. **93**, 177206 (2004).
[22]Z. H. Sun, W. S. Yan, G. B. Zhang, H. Oyanagi, Z. Y. Wu, Q. H. Liu, W. Q. Wu, T. F. Shi, Z. Y. Pan, P. S. Xu, and S. Q. Wei, Phys. Rev. B **77**, 245208 (2008).
[23]S. R. Shinde, S. B. Ogale, J. S. Higgins, H. Zheng, A. J. Millis, V. N. Kulkarni, R. Ramesh, R. L. Greene, and T. Venkatesan, Phys. Rev. Lett. **92**, 166601 (2004).
[24]Q. Liu, C. L. Gan, C. L. Yuan, and G. C. Han, Appl. Phys. Lett. **92**, 032501 (2008).
[25]D. P. Norton, M. E. Overberg, S. J. Pearton, K. Pruessner, J. D. Budai, L. A. Boatner, M. F. Chisholm, J. S. Lee, Z. G. Khim, and Y. D. Park, Appl. Phys. Lett. **83**, 5488 (2003).
[26]P. Vargas, J. D. Castro, and D. Altbir, Phys. Rev. B **60**, 6541 (1999).
[27]S. Q. Zhou, K. Potzger, J. V. Borany, R. Grötzschel, W. Skorupa, M. Helm, and J. Fassbender, Phys. Rev. B **77**, 035209 (2008).

[28]S. Yin, M. X. Xu, L. Yang, J. F. Liu, H. Rösner, H. Hahn, H. Gleiter, D. Schild, S. Doyle, T. Liu, T. D. Hu, E. T. Muromachi, and J. Z. Jiang, Phys. Rev. B **73**, 224408 (2006).
[29]A. Ney, K. Ollefs, S. Ye, T. Kammermeier, V. Ney, T. C. Kaspar, S. A. Chambers, F. Wilhelm, and A. Rogalev, Phys. Rev. Lett. **100**, 157201 (2008).
[30]T. C. Kaspar, T. Droubay, S. M. Heald, M. H. Engelhard, P. Nachimuthu, and S. A. Chambers, Phys. Rev. B **77**, 201303 (2008).
[31]K. Potzger, S. Q. Zhou, J. Grenzer, M. Helm, and J. Fassbender, Appl. Phys. Lett. **92**, 182504 (2008).